Metal Particle Size in Ni/SiO_2 Materials Prepared by Deposition−Precipitation: Influence of the Nature of the Ni(II) Phase and of Its Interaction with the Support

Paolo Burattin,[†] Michel Che,[‡] and Catherine Louis*

Laboratoire de Réactivité de Surface, UMR 7609 CNRS, Université Pierre et Marie Curie, 4 place Jussieu, 75252 Paris Cedex 05, France

Received: January 8, 1999; In Final Form: April 1, 1999

The influence of the parameters of the deposition−precipitation method used to prepare Ni/SiO_2 samples on the size of nickel metal particles was investigated by temperature-programmed reduction, transmission electron microscopy, and thermogravimetry. The results show that the average metal particle size, which varies between 27 and 79 Å, depends on the nature and the reducibility of the supported Ni(II) phase (nickel hydroxide or 1:1 nickel phyllosilicate), and on the extent of the interface between the supported Ni(II) phase and silica. These parameters themselves depend on the characteristics of the silica support (surface area and morphology) and on the preparation parameters (urea and silica concentrations). At the interface, a nickel phyllosilicate is detected whatever the nature of the supported Ni(II) phase. The metal particles are smaller and the size distribution is narrower when the supported phase is a 1:1 nickel phyllosilicate ($\bar{d} \leq 50$ Å, 10−100 Å) than when it is a nickel hydroxide ($\bar{d} \approx 80$ Å, 20−280 Å). The metal particles are smaller when the extent of the Ni(II) phase−silica interface increases. This arises from the comparison of Ni/SiO_2 samples prepared from silicas of high and low surface area, and from nonporous and porous silica.

Introduction

The deposition−precipitation (DP) method used to prepare silica-supported Ni samples[1] consists of precipitating a nickel(II) phase onto silica by basification of a nickel salt solution containing silica in suspension. Urea ($CO(NH_2)_2$) heated at 90 °C enables a gradual and homogeneous basification of the solution and avoids local high pH and the subsequent precipitation of nickel hydroxide in solution.

The advantages of this method of preparation of Ni/SiO_2 catalysts are the following: (a) the metal particles obtained after thermal reduction are smaller and exhibit narrower size distribution than in Ni/SiO_2 samples prepared by impregnation;[2−8] (b) in contrast with samples prepared by cationic exchange, which also leads to small metal particles, it is possible to deposit high nickel loadings (>20 wt %); (c) the metal particles do not easily sinter because of their strong interaction with the support[2,4−12]; and (d) this preparation method is highly reproducible.[2]

In previous papers,[13−15] we showed that the nature of the DP Ni(II) phase and the extent of the interface between the Ni(II) phase and the silica support depend on the characteristics of silica and on the parameters of DP. The goal of the present paper is to investigate the influence of these parameters on the size of the nickel metal particles after thermal-programmed reduction. The nickel metal particles are measured from transmission electron micrographs. The results are discussed on the basis of the mechanism of reduction of the Ni(II) phase supported on silica proposed by Coenen[16] and by Martin et al.,[17] and on the basis of the results already reported in refs 13−15; these results gathered in Table 1 can be summarized as follows: (a) The nickel loading increases with the DP time. In this paper, the DP times are chosen shorter than 4 h so as to get samples with nickel loadings lower than 25 wt %; (b) In the so-called standard conditions of preparation reported in Experimental section and for DP times shorter than 4 h, the DP Ni(II) phase supported on silica of low surface area (≈50 m^2/g) is mainly a nickel hydroxide with a turbostratic structure, i.e., α-$Ni(OH)_2$ with a disordered stacking of brucitic layers (Figure 1a), whereas that on silica of high surface area (≈400 m^2/g) is mainly a 1:1 nickel phyllosilicate (Figure 1b). This compound exhibits a layered structure consisting of a brucite-type sheet containing Ni(II) in octahedral coordination and a sheet containing linked tetrahedral SiO_4 units;[18] (c) The nature of the DP Ni(II) phase is rather similar whether silica is porous or not; the main difference is that the extent of the Ni(II) phase−silica interface is larger with nonporous silica because of the more regular shape of the silica particles; (d) The nature of the DP Ni(II) phase depends on the concentration of the reactants, urea concentration and silica loading, and on the hydrothermal treatments undergone by the samples, which transform 1:1 phyllosilicate into 2:1 phyllosilicate (Figure 1c);[19] (e) The nature of the DP Ni(II) phase and the strength of the Ni(II) phase-support interaction also depend on the nature of the support, as shown in Table 1 when nickel is deposited on alumina and zirconia. It will be shown in the following that it is possible to establish a correlation between the size of the nickel metal particles and (i) the nature of the DP Ni(II) phase, (ii) the extent of the interface between the Ni(II) phase and the support, and (iii) the strength of the Ni(II) phase-support interaction.

Experimental

1. Sample Preparation. The DP Ni/SiO_2 samples were prepared according to the standard procedure described by Hermans and Geus[1] (details can also be found in refs 14, 15, 22): 380 mg of oxide support was put into a vessel thermostated at 90 °C. An aqueous solution (50 mL) containing nickel nitrate (0.14 M), urea (0.42 M) and nitric acid (0.02 M) was added at

[‡] Institut Universitaire de France.

[†] Permanent address: Rhône Poulenc CRIT-Carrières, 86 avenue des Frères Perret, BP 62, 69192 Saint Fons Cedex, France.

10.1021/jp990115t CCC: $18.00 © 1999 American Chemical Society
Published on Web 07/09/1999

TABLE 1: Characteristics of Supported Ni Samples Prepared by Deposition−Precipitation in Standard Conditions (0.14 M of Nickel Nitrate, 0.42 M of Urea, 7.6 g.L^{-1} of Silica), except when Mentioned

samples	support[b]	Ni loading (wt %)[a]	Ni(II) phase[a]	TPR peak max[a,c] (°C)	metal particles: size distr. (Å)	metal particles: $\bar{d}$ (Å)
Ni/XOA400 (70 min)	356 m^2.g, porous	5.2	ϵ(Ni(OH)$_2$) + 1:1 Ni phyllo.	380 (sh) + 460	10−120	53
(2.5 h)		17.2	1:1 Ni phyllo.	510	10−90	47
(4 h)		25.1	1:1 Ni phyllo.	545	10−100	50
Ni/XO30LS (70 min)	44 m^2/g, porous	2.8	Ni(OH)$_2$	380	20−280	78
(2.5 h)		12.5	Ni(OH)$_2$ + ϵ(1:1 Ni phyllo.)	380, 450 (sh)	20−280	79
(4 h)		21.3	Ni(OH)$_2$ + ϵ(1:1 Ni phyllo.)	380, 450−500	10−240	77
Ni/AD380 (2.5 h)	380 m^2.g^{-1}, nonporous	17.2	1:1 Ni phyllo.	530	10−90	37
Ni/XOA400 (2.5 h)	356 m^2.g^{-1}, porous	17.2	1:1 Ni phyllo.	510	10−90	47
Ni/OX50 (2.5 h)	50 m^2.g^{-1}, nonporous	14.7	Ni(OH)$_2$ + 1:1 Ni phyllo.	410, 450−500 (sh)	10−70	27
Ni/XO30LS (2.5 h)	44 m^2.g^{-1}, porous	12.5	Ni(OH)$_2$ + ϵ(1:1 Ni phyllo.)	380, 450 (sh)	10−240	79
Ni/XOA400 (2.5 h) (3.8 g.L^{-1})[d]	356 m^2.g^{-1}, porous	27.8	Ni(OH)$_2$ + 1:1 Ni phyllo	390 + 515	20−160	58
(7.6 g.L^{-1})		17.2	1:1 Ni phyllo.	510	10−90	47
(15.2 g.L^{-1})		9.6	1:1 Ni phyllo.	520, 650 (sh)	20−100	43
Ni/XOA400 (2.5 h) (0.42 M)[e]	356 m^2.g^{-1}, porous	17.2	1:1 nickel phyllo.	510	10−90	47
(0.84 M)		24.6	ϵ(Ni(OH)$_2$) + 1:1 Ni phyllo.	380 (sh), 505	10−80	34
(1.68 M)		33.9	Ni(OH)$_2$ + 1:1 Ni phyllo.	380, 490	10−250	47
Ni/XOA400 (4 h) + HT[f] at 190°C	356 m^2.g^{-1}, porous	23.9	2:1 nickel phyllo.	755	10−80	39
Ni/Al_2O_3 (2.5 h)	73 m^2.g^{-1}	15.3	unsupported Ni(OH)$_2$ + Ni(OH)$_2$ + Ni aluminate	300, 365, 445	10−110	49
Ni/ZrO_2 (2.5 h)	135 m^2.g^{-1}	13.2	unsupported Ni(OH)$_2$	320	50−300	

[a] Results in columns 3, 4 and 5 arise from refs 13−15. [b] Silica, except when mentioned in the first column. [c] Temperature for maximum hydrogen consumption. [d] Silica loading. [e] Urea concentration. [f] HT = hydrothermal treatment.

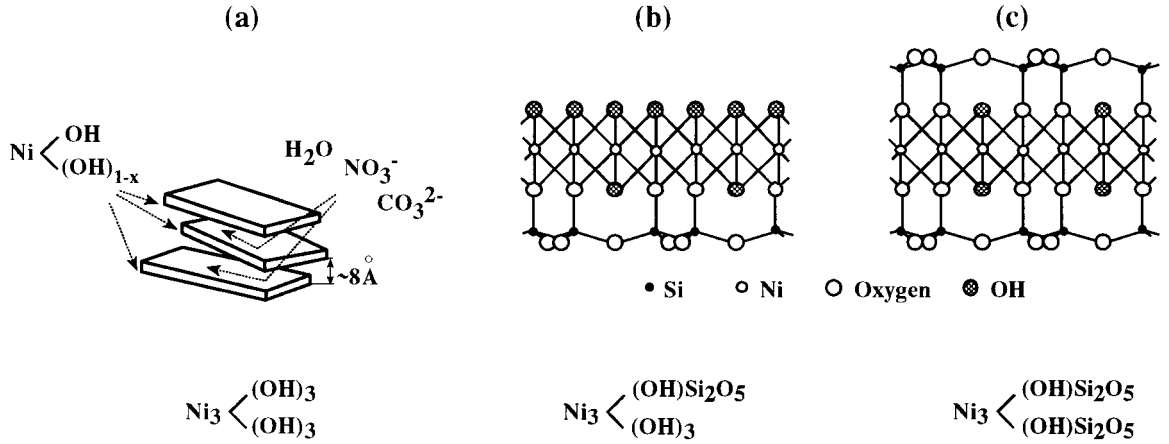

Figure 1. Structure of (a) turbostratic nickel hydroxide (α-Ni(OH)$_2$), from ref 20; (b) a layer of 1:1 nickel phyllosilicate; (c) a layer of 2:1 nickel phyllosilicate (projection on the bc plane), from ref 21.

$t = 0$, and the suspension (7.6 g/L of silica) was magnetically stirred. The solution reached 90 °C within 3 min, during which the deposition−precipitation started. After a given DP time, the suspension was cooled to 20−25 °C and then filtered. The solid was washed three times as follows: after addition of 20 mL of distilled water, the resulting suspension was stirred for 10 min at 50−60 °C before filtration. Finally, the sample was dried at 90 °C for 24 h.

Different silica supports were used: porous and nonporous silicas of low and high surface areas (Table 2). Other supports, Al_2O_3 and ZrO_2, were used as references (Table 2). The notation used for the samples later on is also reported in Table 2.

Nickel nitrate ($Ni(NO_3)_2 \cdot 6H_2O$) was provided by Aldrich (purity >99.0%).

Chemical analyses were performed by inductive coupling plasma in the CNRS Center of Chemical Analysis (Vernaison, France). In the following, the Ni weight loading of the samples is expressed in wt % of Ni per g of sample calcined in air at 1000 °C, the temperature at which nickel phyllosilicates are totally decomposed into NiO and SiO_2:

$$\text{wt \% Ni} = \frac{M_{Ni}}{M_{NiO} + M_{SiO2}} \times 100$$

2. Techniques. After being dried, the samples are reduced without the former calcination treatment according to the following conditions of temperature-programmed reduction (TPR): in a quartz gas flow reactor, from room temperature to 900 °C, with a heating rate of 7.5 °C/min, under a stream of 5% v/v H_2 in argon with a total flow rate of 25 mL/min at atmospheric pressure. The TPR profiles can be found in refs 14 and 15. However, for the sake of clarity, a few of them are reproduced here.

In a former work,[13] the quantitative analysis of H_2 consumed during TPR up to 900 °C revealed only 80−84% of reduction despite the return to the baseline of the TPR profile. The same value was obtained even though the samples were calcined before reduction. Two methods were used to measure the state

TABLE 2: Oxides Used as Supports to Prepare Supported Ni/SiO_2 Catalysts by Deposition−Precipitation

oxide support	origin	characteristics	code for Ni/support
porous silica XOA400	Spherosil, Rhône-Poulenc, France	purity >99.5%, 356 m^2/g, pore volume = 1.25 cm^3/g, average pore diameter = 80 Å	Ni/XOA400 (*t*)[a]
porous silica XO30LS	Spherosil, Rhône-Poulenc, France	purity >99.5%, 44 m^2/g, pore volume = 2.27 cm^3/g, average pore diameter = 1000 Å	Ni/XO30LS (*t*)
nonporous silica AD380	Aerosil, Degussa, Germany	purity >99.95%, 380 m^2/g	Ni/AD380 (*t*)
nonporous silica OX50	Aerosil, Degussa, Germany	purity >99.95%, 50 m^2/g	Ni/OX50 (*t*)
Al_2O_3	Institut Français du Pétrole, France	purity >99.5%, 73 m^2/g	Ni/Al_2O_3 (*t*)
ZrO_2	Rhône-Poulenc, France	purity >99.5%, 135 m^2/g	Ni/ZrO_2 (*t*)

[a] *t* is the DP time.

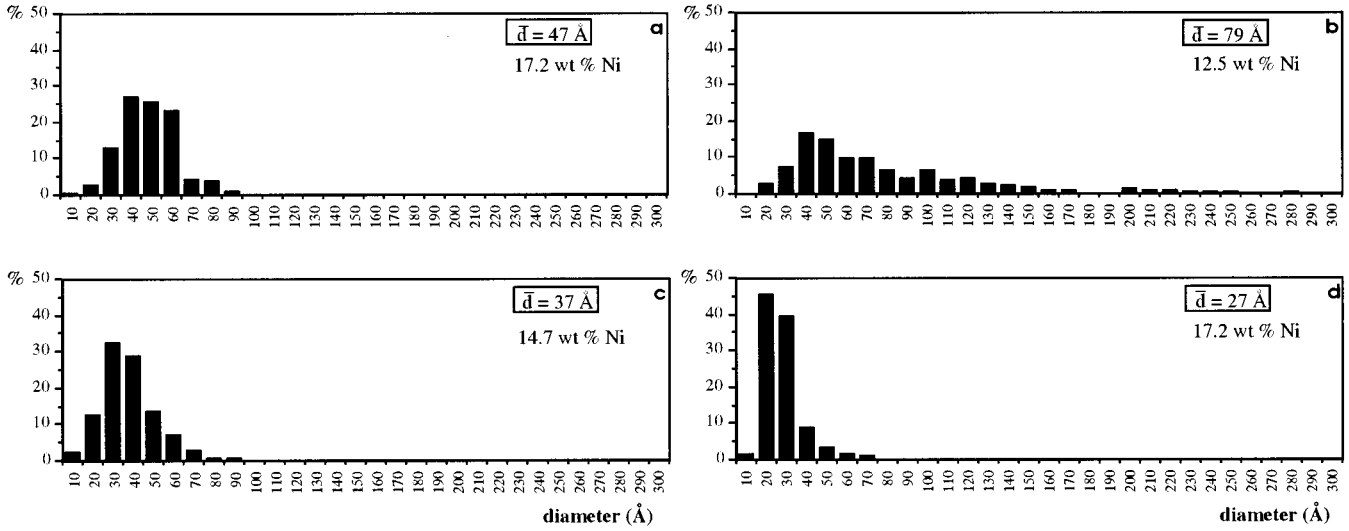

Figure 2. Histograms of metal particle diameters and average diameters of (a) Ni/XOA400; (b) Ni/XO30LS; (c) Ni/AD380; (d) Ni/OX50 prepared by deposition precipitation for 2.5 h and then reduced by TPR up to 900 °C.

of reduction of nickel itself: (i) the chemical method proposed by Coenen,[10] which is based on the measurement of the volume of hydrogen gas generated on dissolution/oxidation of the reduced nickel in sulfuric acid, and (ii) magnetic measurements by the Weiss extraction method.[17] In both cases, the percentages of reduction reached 99−100%. The difference was found to be the result of the high-temperature reduction of part of the nickel without H_2 consumption. Indeed, after a temperature-programmed heating under Ar up to 900 °C, the magnetic measurement revealed a percentage of nickel reduction of 16%. Hence, it could be concluded that nickel was fully reduced after TPR up to 900 °C.[13]

The reduced samples were examined by TEM with a JEOL JEM 100CXII electron microscope equipped with a top-entry device and operating at 100 kV. The histograms of metal particle sizes were established from the measurement of at least 300 particles. The average particle diameter $\bar{d}$ was calculated from the following formula: $\bar{d} = \sum n_i d_i / \sum n_i$ where n_i is the number of particles of diameter d_i. The detection limit is about 10 Å for supported nickel metal particles.

Some samples (40 mg) have been submitted to thermogravimetric analysis (TG) using a Seiko 320 thermobalance under either pure Ar or 5% v/v H_2 in argon with a total flow rate of 25 mL/min, from room temperature to 1000 °C, and with a heating rate of 7.5 °C/min.

Results

Following are reported the results, which show the influence of the parameters involved during the DP preparation on the metal particle size.

1. Influence of the Deposition−Precipitation Time. The particle size distribution and the average diameter ($\bar{d}$) of the metal particles in reduced Ni/XOA400 and Ni/XO30LS samples do not depend on the Ni loading (≈3 to ≈25 wt %), i.e., on the DP time (70 min, 2.5 and 4 h), but are different from one silica support to another (Figure 2 and Table 1). This result differs from that obtained by Richardson and Dubus[2] who observed broader particle size distribution and larger average particle size when the DP time increased. However, under the isothermal reduction conditions they used, under hydrogen at 400 °C for 15 h, nickel was not fully reduced.

2. Influence of the Silica Texture. *Silica Surface Area.* The Ni/XO30LS (≈50 m^2/g) samples exhibit broader particle size distributions (10 to 280 Å) and larger particles ($\bar{d} \approx 80$ Å) than the Ni/XOA400 (≈400 m^2/g) samples (10 to 100 Å, $\bar{d} \approx 50$ Å) (Figure 2 and Table 1).

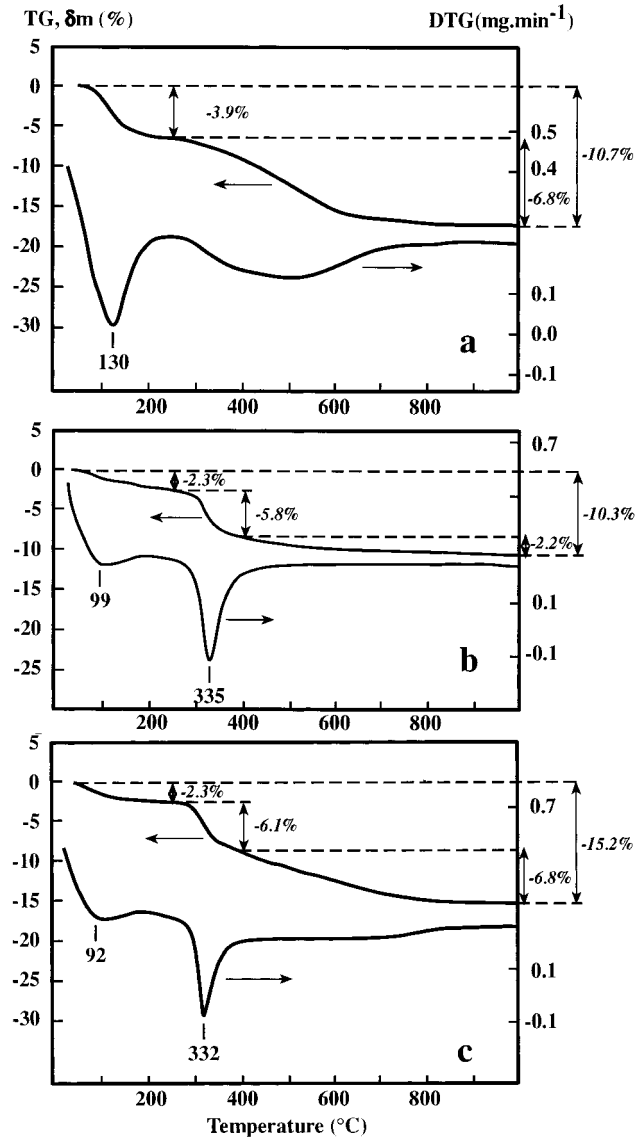

Figure 3. Curves of TG and DTG of (a) Ni/XOA400 (4 h) performed under Ar; (b) Ni/XO30LS (4 h) under Ar; (c) Ni/XO30LS (4 h) under H_2/Ar.

For reasons to be developed in the discussion, the TG analysis of Ni/XOA400 (4 h) and Ni/XO30LS (4 h) was performed under Ar (Figure 3a,b). For both samples, a first weight loss is observed between 60 and 250 °C, and attributed to the desorption of physisorbed and chemisorbed water. It is larger with silica of high surface area because of its higher water adsorption capacity. Beyond 250 °C, the samples behave differently. The weight loss of Ni/XOA400 (4 h) (Figure 3a) gradually increases up to ≈600 °C, whereas the weight loss of Ni/XO30LS (4 h) (Figure 3b) is faster with a maximum of rate at 335 °C and complete at ≈400 °C. The weight losses are attributed to the slow decomposition of the supported phase (Table 1), i.e., nickel phyllosilicate into NiO and SiO_2 for the first sample and nickel hydroxide into NiO for the second one. XRD analysis confirms the formation of NiO at 400 °C for Ni/XO30LS.

When TG of Ni/XO30LS (4 h) is performed under H_2/Ar to reproduce the TPR conditions, the TG curve beyond 400 °C (Figure 3c) is different from that under Ar (Figure 3b). Under H_2/Ar, the sample loses weight up to ≈800 °C, and the weight loss between 400 and 1000 °C is more important than under pure Ar (Figure 3). The difference in weight loss in this temperature range (6.8% − 2.2% = 4.6%) is assigned to the reduction of NiO arising from nickel hydroxide decomposition. The weight loss between 250 and 400 °C is close to that obtained under Ar (Figure 3b,c), indicating that the decomposition of nickel hydroxide into NiO, also occurs between 250 and 400 °C in the presence of hydrogen. The difference of weight loss between the two experiments, i.e., 6.1%−5.8%, is attributed to the reduction of some NiO. However, most of the NiO is reduced above 400 °C. It may be concluded that decomposition and reduction of supported nickel hydroxide on XO30LS do not occur simultaneously. It may be noted that the weight loss calculated for the full reduction of the nickel is 5.7% whereas that measured is smaller: $\delta m = 4.6\% + (6.1\% - 5.8\%) = 4.9\%$, indicating an incomplete reduction during the TG experiments. This may be due to the fact that the reduction gas does not pass through the sample bed but licks at the surface.

Silica Porosity. When nickel is deposited on nonporous silicas, AD380 and OX50, for 2.5 h, the metal particles exhibit narrower size distributions with smaller average size ($\bar{d}$ = 37 and 27 Å, respectively) (Figure 2c,d and Table 1) than on porous silicas, XOA400 and XO30LS, ($\bar{d}$ = 47 and 79 Å, respectively) (Figure 2a,b and Table 1). The difference in average particle size is more drastic when one compares silicas of low surface area (≈50 m^2/g) than when one compares silicas of high surface area (≈400 m^2/g). The difference in size distribution is also striking since the largest particles reach 280 Å in Ni/XO30LS and 70 Å in Ni/OX50 (Table 1).

3. Influence of the Reactant Concentration. When the urea concentration is larger (0.84; 1.68 M) than that used in the standard conditions (0.42 M), the Ni loading in Ni/XOA400 (2.5 h) increases (17.2, 24.6, 33.9 wt % Ni) as discussed earlier.[15] The average metal particle size decreases from 47 to 37 Å when the concentration increases from 0.42 to 0.84 M, and increases again (47 Å) for the 1.68 M concentration, because of the presence of large particles (100−250 Å) (Table 1) not observed at lower urea concentrations.

When the silica loading increases in the suspension (3.8, 7.6, and 15.2 g/L), the Ni loading in Ni/XOA400 (2.5 h) decreases (27.8, 17.2, 9.6 wt % Ni).[15] Simultaneously, the average metal particle size decreases from 58 to 43 Å and the size distribution becomes narrower (Table 1).

4. Influence of the Hydrothermal Treatment. The Ni/XOA400 (4 h) sample submitted to a hydrothermal treatment at 190 °C for 7 days before reduction[13,14] exhibits a narrower size distribution and smaller average metal particles (Table 1) (Figure 4b) than without hydrothermal treatment (50 Å) (Figure 4a).

5. Influence of the Nature of the Oxide Support. After reduction of Ni/Al_2O_3 (2.5 h) by TPR up to 900 °C, the particle size distribution and the average metal particle size (49 Å) are close to those in Ni/XOA400 (2.5 h) (47 Å) (Table 1). For the Ni/ZrO_2 (2.5 h) sample, the contrast between the nickel metal particles and the zirconia support is poor on the electron micrographs, and the only visible nickel particles were those located on the side of the support particles. They exhibit large sizes between 50 and 300 Å.

Discussion

Despite the complexity of the data gathered in Table 1, some correlations can be established between the average size of the nickel metal particles and the following parameters: (i) the nature and reducibility of the DP Ni(II) phase; (ii) the extent of the interface between the Ni(II) phase and silica; (iii) the strength of the Ni(II) phase-support interaction.

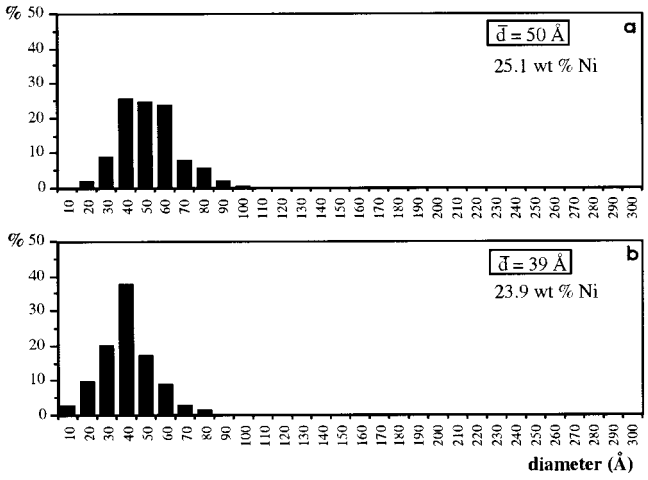

Figure 4. Histograms of metal particle diameters and average diameters of (a) Ni/XOA400 (4 h); (b) Ni/XOA400 (4 h) submitted to a hydrothermal treatment at 190 °C for 7 days.

1. Nature and Reducibility of the DP Ni(II) Phase. Table 1 shows that the Ni/SiO_2 samples containing mainly nickel hydroxide before reduction (reduction peak at ≈380 °C) exhibit metal particles with broader size distributions and larger average sizes than the samples containing mainly 1:1 nickel phyllosilicate (reduction peak at ≈500 °C).

This is also exemplified by a set of Ni/SiO_2 (4 h) samples in Table 1 whose Ni loading is about the same (≈20 wt % Ni) but whose DP Ni(II) phase is different: a nickel hydroxide in Ni/XO30LS (4 h), a 1:1 nickel phyllosilicate in Ni/XOA400 (4 h), and a 2:1 nickel phyllosilicate after hydrothermal treatment at 190 °C. Table 1 and Figure 5 show that upon changes in the nature of the Ni(II) phase along the above sequence, the Ni(II) phase is reduced at increasing temperature, i.e., its reducibility decreases, and the average metal particle size decreases.

The dependence of the nickel metal particle size on the precursor reducibility is usually accepted in the literature:[8,23,24] the lower the reducibility, the smaller the nickel metal particles. To explain this correlation, Martin et al.[17] proposed a mechanism of reduction for Ni/SiO_2 samples prepared by cation exchange with nickel hexaammine complexes reported in Figure 6; this mechanism is also based on Coenen's work on Ni/SiO_2 samples prepared by DP.[16]

It may be noted that according to these authors,[16,17] the supported phase was supposed to be $Ni(OH)_2$ interacting with silica via a silicate intermediate at the interface. However, more recent works showed that 1:1 nickel phyllosilicate is the main Ni(II) phase formed in Ni/SiO_2 samples prepared either by exchange with nickel hexaammine complexes[25,26] or by DP on silica of high surface area.[1,10,11,14,27−29] This suggests that the mechanism of reduction proposed by Martin et al. also applies to supported nickel phyllosilicates.

So, according to Martin et al. and Coenen,[16,17] the very first step of the mechanism of reduction is the dehydration of the supported Ni(II) phase into a two-dimensional NiO phase (step 1 in Figure 6). It takes place whether or not the reduction treatment is preceded by a vacuum thermal treatment. According to Coenen,[16] no significant structural change occurs during this step (300−550 °C), apart from the direct effect of dehydration. Then, depending on the conditions, the mechanism of reduction either passes through a step of NiO sintering, during which NiO becomes three-dimensional (step 2) before it is reduced into Ni^0 (step 4), or takes place in one single step (step 3). The step of NiO sintering (step 2) is slow and water-sensitive. Reduction

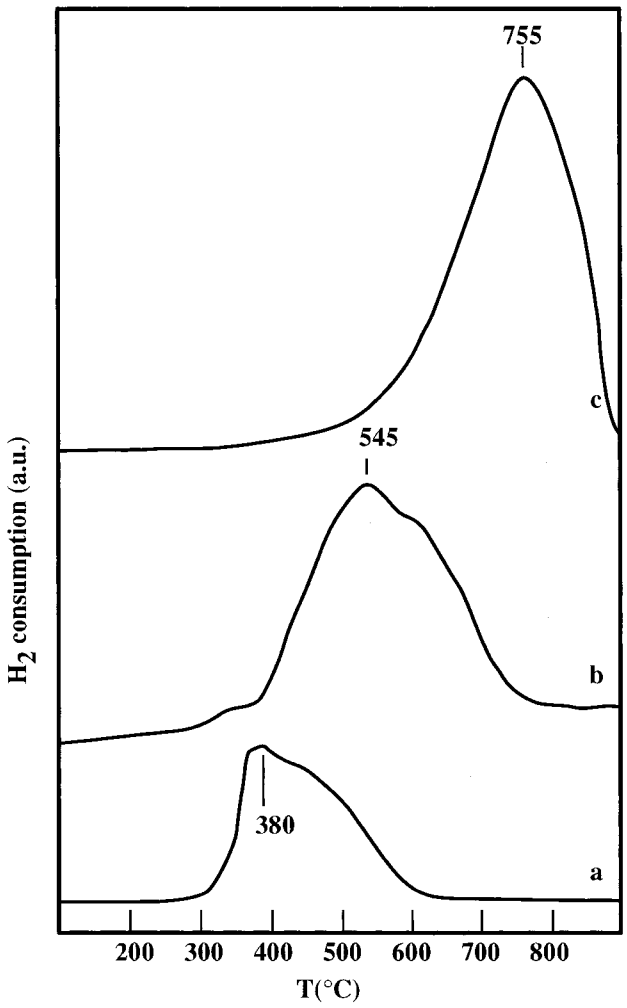

Figure 5. TPR profiles of (a) Ni/XO30LS (4 h); (b) Ni/XOA400 (4 h); (c) Ni/XOA400 (4 h) submitted to a hydrothermal treatment at 190 °C for 7 days.

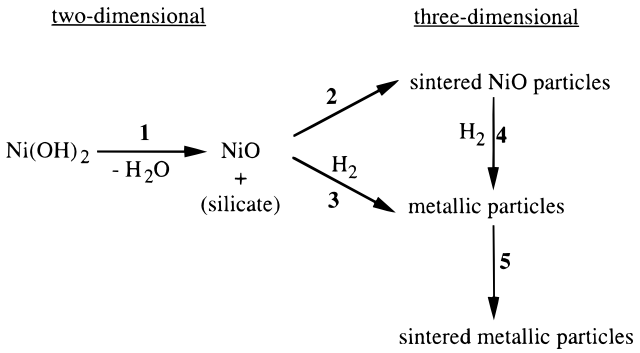

Figure 6. Mechanism of reduction of silica-supported nickel samples, from ref 17.

of NiO into Ni^0 (step 3 or 4) does not imply nickel mass transfer and occurs via a nucleation step, which is rate-determining for the reduction, according to Coenen.[16] Propagation of the reduction front is very fast in the oxide crystallites. The nucleation step may be water-poisoned and is hydrogen-sensitive. So, if water is removed with a high gas flow rate, a slow heating rate, or a thermal pretreatment under vacuum, or if the pressure of H_2 is high, step 3 is favored over step 2, and a better metal dispersion is obtained. Metal sintering (step 5) may occur when reduction is performed at high temperature (>600 °C) and for a long time. The relevant feature in this mechanism of reduction (Figure 6) is that reduction takes place

once the Ni(II) precursors are decomposed (step 1), even though reduction is performed in a single process (step 3). This is confirmed by the thermogravimetry experiments performed on Ni/XO30LS (4 h) under Ar and under H_2/Ar (Figure 3b,c), and discussed above in section Results 2.

If one considers the decomposition of the different Ni(II) phases present in our DP Ni/SiO_2 samples, previous DTA experiments show that it occurs as follows:[21,30−32]

nickel hydroxide < 1:1 nickel phyllosilicate < 2:1 nickel phyllosilicate
(≈300 °C) (≈600 °C) (≈900 °C)

Although the presence of a support usually modifies the decomposition temperature, this order is not changed by the presence of silica as confirmed by our TG experiments (Figure 3a,b): supported nickel hydroxide, the main Ni(II) phase in Ni/XO30LS (4 h), decomposes between 250 and 400 °C, whereas supported 1:1 nickel phyllosilicate, the main Ni(II) phase in Ni/XOA400 (4 h), decomposes between ≈300 and 600 °C. As mentioned above, since the decomposition of the Ni(II) phase into oxides precedes the reduction, one can deduce that the higher the decomposition temperature, the higher the reduction temperature. This was also observed by Martin et al.[21] with 1:1 and 2:1 bulk nickel phyllosilicates. In addition, the higher the decomposition temperature, the more efficiently water is eliminated from the sample before reduction. In consequence, reduction of nickel via step 3 is favored over reduction via steps 2 and 4 in Figure 6, and for the same reason, sintering of the oxide phase (step 2) is not favored. This reasoning can explain the correlation found in the literature for the Ni/SiO_2 system:[8,23,24] the lower the reducibility, the smaller the metal particles; this correlation applies to our results (Table 1, Figure 5).

The differences in metal particle size could also be due to the fact that the particles of the NiO intermediate after step 1 are smaller when they arise from nickel phyllosilicate decomposition than from $Ni(OH)_2$ decomposition. Indeed, according to Coenen,[16] there is no mass transfer during reduction, and one oxide crystallite produces one nickel metal crystallite. This interpretation does not contradict that given just above.

It could also be argued that the differences in metal particle size are due to different extents of metal particle sintering (step 5) within the temperature interval (ΔT) between the end of the nickel reduction and the end of the TPR experiment at 900 °C. Here, ΔT increases as follows: nickel hydroxide > 1:1 nickel phyllosilicate > 2:1 nickel phyllosilicate (Figure 5). However, this hypothesis can be ruled out since it will be shown below that there is no significant sintering after the reduction is complete.

In consequence, the decrease in the average particle size, according to the 2:1 nickel phyllosilicate < 1:1 nickel phyllosilicate < nickel hydroxide sequence is attributed to the fact that the higher the decomposition temperature of the Ni(II) phase, the lower the amount of water still present in the sample after decomposition, so, the lower the NiO sintering and the faster the reduction.

2. Extent of the Interface between the Ni(II) Phase and Silica. *Silica Surface Area*. The various nature of the DP Ni(II) phase is not the only reason for the different average metal particle sizes after reduction. Other reasons must be found to explain that for each set of Ni/XOA400 and Ni/XO30LS samples prepared with different DP times (70 min, 2.5 and 4 h); the metal particle size does not vary although the nature of the DP Ni(II) phase evolves with time (Table 1).

In our previous study,[14] it was shown by TEM that the DP Ni(II) phase in Ni/XOA400 and Ni/XO30LS samples (≤ 4 h) exhibited drastic differences in morphology and distribution onto the support. A large number of small and thin platelets of 1:1 nickel phyllosilicate (stacks of 2−5 layers) with random orientations covered the surface of silica XOA400, whereas a restricted number of larger and thicker stacks of nickel hydroxide layers, nonhomogeneously dispersed on silica XO30LS, left some parts of silica uncovered. It was deduced[14,15] that the interface between the Ni(II) phase and the support was less extended for silica XO30LS than for silica XOA400. Hence, it seems that the less extended the Ni(II) phase−silica interface, the larger the metal particles. It may be added that this interface has been proposed to consist of a brucitic layer of octahedral Ni(II) bonded to the silica surface, forming with silica a sheet of 1:1 nickel phyllosilicate[11,14−16]; it is the same whether the Ni(II) phase is an hydroxide or a 1:1 phyllosilicate.

Porosity of Silica. When nickel is supported on nonporous silicas, OX50 (≈50 m^2/g) and AD380 (≈400 m^2/g), smaller metal particles with narrower size distribution are obtained compared to porous silicas, XO30LS (≈50 m^2/g) and XOA400 (≈400 m^2/g), respectively (Table 1). This is despite the fact that the nature of the Ni(II) phase does not strongly depend on the porosity of silica (Table 1). In a previous study,[14] TEM showed that the DP Ni(II) phase better follows the shape of the particles of nonporous silica than of porous silica because of the more regular shape of the particles. In other words, the DP Ni(II) phase better interacts with nonporous silica and the interface is more extended than with porous silica. The consequences are that the DP Ni(II) phase is better crystallized[14] and is slightly less reducible (Table 1), which leads to smaller metal particles.

According to characterization studies reported in refs 13 and 14, the proportion of 1:1 nickel phyllosilicate is higher in Ni/OX50 than in Ni/XO30LS. This is probably also a reason for which the metal particle sizes are so different (27 and 79 Å).

It can be noted that despite the fact that the reduction of the Ni(II) phase on silica OX50 is complete at 650 °C and that the TPR proceeds up to 900 °C, this sample provides the smallest average metal particle size (27 Å). This indicates that the sintering of Ni^0 (step 5 in Figure 6) is probably not important between 650 and 900 °C. The resistance to sintering of the metal particles in DP Ni/SiO_2 samples is reported in the literature (see Introduction section) and is confirmed by the following experiment: the size of the metal particles does not change when the Ni/XOA400 (4 h) sample reduced by TPR up to 900 °C is maintained for 1 h under H_2/Ar at 900 °C.

3. Strength of the Ni(II) Phase−Support Interaction. The results in Table 1 also show that for the same DP time and Ni loading, the metal particle size and the size distribution depend on the nature of the support. If one compares Ni/ZrO_2 (2.5 h) with Ni/XO30LS (2.5 h), the Ni(II) phase is a nickel hydroxide in both cases (Table 1). However, the metal particle sizes are larger in Ni/ZrO_2 (50−300 Å) than in Ni/XO30LS (20−280 Å). The difference is attributed to different strength of the Ni(II) phase−support interaction. Indeed, nickel hydroxide is bonded to the silica support whereas it does not seem to interact with ZrO_2, as attested by the TPR profile of Ni/ZrO_2 (Table 1), which looks like that of unsupported nickel hydroxide (single peak at 300 °C).[13]

In contrast, if one compares Ni/Al_2O_3 (2.5 h) with Ni/XOA400 (2.5 h) and Ni/XO30LS (2.5 h), the nature of the DP

Ni(II) phase is not the same (Table 1). As mentioned above, there is strong evidence that nickel phyllosilicate is located at the Ni(II) phase−support interface, when the Ni(II) phase is a nickel hydroxide and *a fortiori* a nickel phyllosilicate.[11,14−16] This is probably also true for nickel aluminate in Ni/Al_2O_3, as suggested by Morikawa et al.[33]

These results show that the metal particle size depends on the nature of the support. This also means that the particle size depends on the strength of the Ni(II) phase−support interaction, i.e., on the presence or absence at the interface of a mixed surface compound involving cations of the support.

It is generally accepted in the literature[5,7,34,35] that the stronger the nickel−support interaction, the smaller the metal particle size generated by thermal reduction. However, it is not always clear whether the nickel−support interaction refers to the Ni(II) or Ni(0) phase. According to several authors,[23,36,37] metal particles are not fully reduced after reduction, and unreduced or nonfully reduced ions would be located at the metal−support interface. This was demonstrated by Huizinga and Prins[36] in the case of the Pt/TiO_2 and Pt/Al_2O_3 systems; they showed by ESR that Pt^+ ions are located at the metal−support interface. Bonneviot et al.[37] also showed by ESR and DRS that Ni^+ and/or Ni^{2+} ions are located at the nickel−silica interface. CNDO/2 and EHMO calculations on the interaction between Ni atoms and surface clusters of oxide supports are consistent with these results:[38,39] in the case of a completely oxidized support surface such as SiO_2, it was found that the nickel net charge is positive, indicating an electron transfer to the support.

Hence, it is suggested that all of the Ni ions of the Ni(II) phase−support interface, i.e., in the mixed surface compound, nickel phyllosilicate or nickel aluminate, are not reduced. These ions bonded to the silica surface would probably act as anchoring sites for the metal particles, leading to their stabilization, and favoring the metal dispersion. It may be reminded that the quantitative analysis of the reduction state of nickel after TPR indicated that all of the nickel is reduced (see Experimental section); the amount of these unreduced ions is probably too low to be detected.

4. Key Parameters. It is not straightforward to interpret the dependence of the silica loading and the urea concentration on the particle size since, simultaneously, the nature and the reducibility of the DP Ni(II) phase change (Table 1). The relevant feature is that when nickel hydroxide is present in significant proportion in the DP Ni(II) phase, the size distribution is broader and the average metal particle size larger, in agreement with the other results.

According to the present work, the key parameters to control the size of supported metal particles in DP Ni/SiO_2 samples appear to be the nature of the supported phase before reduction, the extent of the interface between the Ni(II) phase, and the support and the strength of the Ni(II) phase−support interaction. All of these parameters have an influence on the reducibility of the supported Ni(II) phase.

To obtain small metal particles in Ni/SiO_2 samples prepared by DP, it is recommended (i) to deposit 1:1 nickel phyllosilicate rather than nickel hydroxide; and (ii) to use a nonporous silica, so as to increase the extent of the Ni(II) phase−silica interface. Small metal particles can also be obtained if, prior to reduction, the sample is submitted to a hydrothermal treatment, which transforms supported 1:1 nickel phyllosilicate into 2:1 nickel phyllosilicate.

According to the literature,[5−7,9] the metal particles are smaller in Ni/SiO_2 samples prepared by DP than by impregnation. In Ni/XOA400 samples prepared by impregnation with nickel nitrate,[40] the metal particles obtained after reduction by TPR up to 700 °C exhibit an average particle size of ≈65 Å, whatever the Ni loading (1.5−35 wt % Ni). In DP Ni/XOA400, whose Ni(II) phase is a 1:1 nickel phyllosilicate, the average metal particle size (<50 Å) is smaller than in impregnated samples, in agreement with literature data.[5−7,9] However, when the DP Ni(II) phase is a nickel hydroxide (Ni/XO30LS), the average metal particle size (≈80 Å) is about the same as in the impregnated samples. This is probably due to the fact that the supported Ni(II) phases, nickel hydroxide and nickel nitrate, are reducible at almost the same temperature, and that the same type of Ni(II) phase−silica interaction is involved owing to the presence of nickel phyllosilicate at the interface; this interface is also known to be formed in impregnated Ni/SiO_2 samples during the drying step at about 90 °C.[40] The different particle sizes in DP Ni/XOA400 and impregnated Ni/XOA400 probably arise from the fact that nickel phyllosilicate is reduced at higher temperature than nickel nitrate.

Conclusion

This paper deals with the influence of the conditions of preparation by DP of Ni/SiO_2 samples on the nickel metal particle size after TPR up to 900 °C. The results show that the average size of the nickel metal particles in Ni/SiO_2 samples obtained after 2.5 h of DP varies within a rather large range, from 27 to 79 Å, for rather close Ni loadings (12.5 to 17.2 wt % Ni) when the characteristics of the silica support (surface area and porosity) and the preparation parameters (urea and silica concentrations) change. These changes have been attributed to the different nature and reducibility of the DP Ni(II) phase, the different extent of the interface between the Ni(II) phase and the support, and the different strength of the Ni(II) phase−support interaction. The Ni(II) phase−silica interface probably consists of nickel phyllosilicate whether the DP Ni(II) phase is a nickel hydroxide or a nickel phyllosilicate. On the basis of other works,[36−38] it is suggested that after reduction, all of the Ni ions of the interface are not fully reduced and act as anchoring sites for the metal particles.

The results presented here also show that the conditions required to get small metal particles after reduction are the following: (a) reducibility of the metal precursor at high temperature; (b) existence of a strong metal precursor−support interaction; (c) large extent of the metal precursor−support interface.

Acknowledgment. The authors are indebted to Rhône Poulenc (France) for financial support of this work.

References and Notes

(1) Hermans, L. A. M.; Geus, J. W. In *Preparation of Catalysts II*; Delmon, B., Grange, P., Jacobs, P. A., Poncelet, G., Eds.; Elsevier: Amsterdam, 1979; p 113.

(2) Richardson, J. T.; Dubus, R. J. *J. Catal.* **1978**, *54*, 207.

(3) Richardson, J. T.; Dubus, R. J.; Crump, J. G.; Desai, P.; Osterwalder, U.; Cale, T. S. In *Preparation of Catalysts II*; Delmon, B., Grange, P., Jacobs, P. A., Poncelet, G., Eds.; Elsevier: Amsterdam, 1979; p 131.

(4) Montes, M.; Soupart, J. B.; de Saedeleer, M.; Hodnett, B. K.; Delmon, B. *J. Chem. Soc., Faraday Trans. 1* **1984**, *80*, 3209.

(5) Blackmond, D. A.; Ko, E. I. *Appl. Catal.* **1984**, *13*, 49.

(6) Delmon, B. *J. Mol. Catal.* **1990**, *59*, 179.

(7) Gil, A.; Diaz, A.; Gandia, L. M.; Montes, M. *Appl. Catal. A* **1994**, *109*, 167.

(8) Keane, M. A. *Can. J. Chem.* **1994**, *72*, 372.

(9) Montes, M.; Penneman de Bosscheyde, C.; Hodnett, B. K.; Delannay, F.; Grange, P.; Delmon, B. *Appl. Catal.* **1984**, *12*, 309.

(10) Coenen, J. W. E. *Appl. Catal.* **1989**, *54*, 65.

(11) Coenen, J. W. E. *Appl. Catal.* **1991**, *75*, 193.

(12) Martra, G. M.; Swaan, H. M.; Mirodatos, C.; Kermarec, M.; Louis, C. *Stud. Surf. Sci. Catal.* **1997**, *111*, 617.
(13) Burattin, P. Ph.D. Thesis, Université Pierre et Marie Curie, Paris, 1994.
(14) Burattin, P.; Che, M.; Louis, C. *J. Phys. Chem. B* **1997**, *101*, 7060.
(15) Burattin, P.; Che, M.; Louis, C. *J. Phys. Chem. B* **1998**, *102*, 2722.
(16) Coenen, J. W. E. In *Preparation of Catalysts II*; Delmon, B., Grange, P., Jacobs, P. A., Poncelet, G., Eds.; Elsevier: Amsterdam, 1979; p 89.
(17) Martin, G. A.; Mirodatos, C.; Praliaud, H. *Appl. Catal.* **1981**, *1*, 367.
(18) 1:1 nickel phyllosilicate: layered compound of structural formula $Si_2Ni_3O_5(OH)_4$, also called serpentine, or Ni-lizardite or nepouite when the layers are planar, Ni-antigorite when the layers are splintery, or Ni-chrysotile when they are curled into cylindrical rolls.
(19) 2:1 nickel phyllosilicate: layered compound of structural formula $Si_4Ni_3O_{10}(OH)_2$ when it is well-crystallized, also called Ni-talc or willemseite. The layers consist of two sheets of linked SiO_4 units, which sandwich the brucite-type sheets.
(20) Génin, P.; Delahaye-Vidal, A.; Protemer, F.; Tekaia, F.; Figlarz, M. *Eur. J. Solid State Inorg. Chem.* **1991**, *28*, 505.
(21) Martin, G. A.; Renouprez, A.; Dalmai-Imelik, G.; Imelik, B. *J. Chim. Phys.* **1970**, *67*, 1149.
(22) Burattin, P.; Louis, C.; Che, M. *J. Chim. Phys.* **1995**, *92*, 1377.
(23) Turlier, P.; Praliaud, H.; Moral, P.; Martin, G. A.; Dalmon, J. A. *Appl. Catal.* **1985**, *19*, 287.
(24) Verhaak, M. J. F. M.; van Dillen, A. J.; Geus, J. W. *Appl. Catal. A* **1994**, *105*, 251.
(25) Clause, O.; Kermarec, M.; Bonneviot, L.; Villain, F.; Che, M. *J. Am. Chem. Soc.* **1992**, *114*, 4709.
(26) Che, M.; Cheng, Z. X.; Louis, C. *J. Am. Chem. Soc.* **1995**, *117*, 2008.
(27) van Dillen, J. A.; Geus, J. W.; Hermans, L. A.; van der Meijden, J. In *Proceedings of the 6th International Congress on Catalysis, London, 1976*; Bond, G. C., Wells, P. B., Tompkins, F. C., Eds.; The Chemical Society: London, 1977; Vol. 2, p 677.
(28) de Roos, G.; Fluit, J. M.; Hermans, L. A. M.; Geus, J. W. *Z. Anorg. Allg. Chem.* **1979**, *449*, 115.
(29) Clause, O.; Bonneviot, L.; Che, M.; Dexpert, H. *J. Catal.* **1991**, *130*, 21.
(30) van Eijk van Voorthuysen, J. J. B.; Franzen, P. *Recl. Trav. Chim.* **1951**, *70*, 793.
(31) Wendt, H. *Chimia* **1973**, *27*, 575.
(32) Wendt, G.; Siegel, H.; Schmitz, W. *Cryst. Res. Technol.* **1982**, *17*, 1435.
(33) Morikawa, K.; Shirasaki, T.; Okada, M. *Adv. Catal.* **1969**, *20*, 97.
(34) Uchiyama, S.; Obayashi, Y.; Hayasaka, T.; Kawata, N. *Appl. Catal.* **1989**, *47*, 155.
(35) Keane, M. A.; Patterson, P. M. *J. Chem. Soc., Faraday Trans.* **1996**, *92*, 1413.
(36) Huizinga, T.; Prins, R. *J. Phys. Chem.* **1983**, *87*, 173.
(37) Bonneviot, L.; Che, M.; Olivier, D.; Martin, G. A.; Freund, E. J. *J. Phys. Chem.* **1986**, *90*, 2112.
(38) Haberlandt, H.; Ritschl, F. *J. Phys. Chem.* **1986**, *90*, 4322.
(39) Che, M.; Masure, D.; Chaquin, P. *J. Phys. Chem.* **1993**, *97*, 9022.
(40) Louis, C.; Cheng, Z. X.; Che, M. *J. Phys. Chem.* **1993**, *97*, 5703.